Article

Not peer-reviewed version

Cloning and Functional Analysis of *Nt*HDR in 'Jinzhanyintai' of *Narcissus tazetta var. chinensis* M.Roem

Xiaomeng Hu , Na Zhang , Ke Ke Fan , Yan ting Chang , Bo Wen Zhang , Yun Ya Deng , Hua Shu Wang , Tao Hu * , Jun Yan Ma *

Posted Date: 18 July 2023

doi: 10.20944/preprints202307.1182.v1

Keywords: Chinese Narcissus 'Jinzhanyintai'; floral scent; HDR; GC-MS; transgenic Nicotiana benthamiana

Article

Cloning and Functional Analysis of *NtHDR* in 'Jinzhanyintai' of *Narcissus tazetta var. chinensis* M.Roem.

Xiaomeng Hu [1,2,†], Na Zhang [1,2,†], Keke Fan [1,2], Yanting Chang [1,2], Wenbo Zhang [1,2], Yayun Deng [1,2], Shuhua Wang [1,2], Tao Hu [1,2,*] and Yanjun Ma [1,2,*]

[1] International Center for Bamboo and Rattan, No. 8, Futong Eastern Avenue, Wangjing Area, Chaoyang District, Beijing 100102, China; 15713711540@126.com (X.H.); zhangna402265@163.com (N.Z.); fankk@icbr.ac.cn (K.F.); changyanting@icbr.ac.cn (Y.C.); wenbozhang@icbr.ac.cn (W.Z.); yayundeng@icbr.ac.cn (Y.D.); wang201170@126.com (S.W.)

[2] Key Laboratory of National Forestry and Grassland Administration/Beijing for Bamboo & Rattan Science and Technology, No. 8, Futong Eastern Avenue, Wangjing Area, Chaoyang District, Beijing 100102, China

* Correspondence: hutao@icbr.ac.cn (T.H.); mayanjun@icbr.ac.cn (Y.M.)

Abstract: The key enzyme, 1-hydroxy-2-methyl-2-(E)-butenyl-4-pyrophosphate reductase HDR, responsible for the final step in the MEP pathway, was successfully cloned from the petals of Narcissus tazetta var. chinensis, herein referred to as *NtHDR* (accession number OQ739816). NtHDR exhibits a full-length coding sequence spanning 1380 base pairs, encoding a total of 460 amino acids. Through phylogenetic tree analysis, it has been determined that *NtHDR* shared the closest evolutionary relationship with monocotyledons, specifically *Asparagus officinalis* and *Zingiber officinale*. Utilizing quantitative real-time PCR analysis, it was observed that *NtHDR* exhibited significant expression in both petals and corona, with expression levels varying throughout the flowering process of Narcissus. Specifically, in petals, *NtHDR* expression demonstrated a pattern of initial increase followed by subsequent decrease, while in corona, it consistently increased. Subsequent subcellular localization experiments indicated that *NtHDR* was localized within the chloroplasts. To investigate the functional impact of *NtHDR*, stable transformation was performed, where *NtHDR* was introduced into Nicotiana benthamiana. The resulting transgenic *N. benthamiana* flowers were analyzed using solid-phase microextraction coupled with gas chromatography–mass spectrometry (SPME-GC-MS) to characterize their volatile components. The analysis revealed the presence of the monoterpene compound linalool, as well as the phenylpropanoids benzyl alcohol and phenylethanol, within the floral fragrance components of the transgenic *N.benthamiana* plants. However, these compounds were absent in the floral fragrance components of wild-type tobacco plants, thus highlighting the impact of *NtHDR* transformation on the floral scent profile.

Keywords: Chinese Narcissus 'Jinzhanyintai'; floral scent; HDR; GC-MS; transgenic *Nicotiana benthamiana*

1. Introduction

Floral fragrance consists of a diverse range of volatile organic compounds (VOCs) [1]. In defense against pathogens, parasites, and herbivores, as well as for attracting pollinators, plants release a vast amounts of phytogenic VOCs [2]. Terpenes represent a pivotal class of plant volatiles, and their metabolic pathways have been extensively elucidated. The precursors of terpenoids, including Isopentenyl pyrophosphate (IPP) and dimethylallyl diphosphate (DMAPP), are synthesized through two distinct routes: the cytoplasmic mevalonate pathway and the plastid-localized methylerythritol 4-phosphate pathway (MEP). Subsequently, terpenoids are generated via the catalytic actions of various terpene synthases [3–6]. Notably, the MEP pathway predominantly governs the biosynthesis of monoterpenes [7], which undergo a seven-step enzymatic reaction, where 1-hydroxy-2-methyl-2-

 doi:10.20944/preprints202307.1182.v1

(E)-butenyl-4-diphosphate reductase (HDR) serves as the final step of the reaction catalase. This last catalytic step precisely regulates the production of IPP and DMAPP mixtures [8–10]. Variations in HDR expression have been demonstrated to correlate significantly with alterations in terpene metabolite levels. Studies involving Solanum lycopersicum and Arabidopsis thaliana seeds demonstrated that increased HDR expression led to a corresponding increase in tetra-terpenoid carotenoid content [11]. Furthermore, anatomical investigations of HDR-silenced *Nicotiana tabacum* leaves have revealed the structural disarray in fenestrated tissue accompanied by a reduction in plastid numbers [12]. In the study of metabolic engineering for the valuable terpenoid tanshinone [13], HDR overexpression was proved to indirectly or directly facilitate the accumulation of these terpenoids. In summary, HDR genes can exert indispensable regulatory roles in plant growth and development, with their overexpression resulting in substantial elevation of indirect precursor levels. This can contribute to the upregulation of biosynthesis pathways for numerous downstream products within the MEP pathway [14].

Chinese Narcissus (*Narcissus tazetta* var. *chinensis* M.Roem.), a renowned traditional flower in China, has been cultivated for millennia and is esteemed for its lush green leaves, graceful blossoms, enchanting fragrance, and exceptional ornamental value [15]. Among its significant cultivars, 'Jingzhanyintai' holds a special place. Extensive previous investigations [16–22] have revealed that the primary components of the floral fragrance volatiles in Chinese Narcissus 'Jingzhanyintai' encompass terpenoids and phenylpropanoids, including monoterpene ocimene, linalool, methyl benzoate, and ethyl benzoate. In recent years, although research on key genes involved in the metabolic pathway of Chinese Narcissus floral fragrance has become an increasing concentration [17,23–28], studies that specifically aim to address the HDR remain unreported. To address this knowledge gap, we conducted a comprehensive study where the HDR gene was successfully cloned from the petals of Chinese Narcissus 'Jingzhanyintai' using RT-PCR, leveraging transcriptome data. Subsequent subcellular localization experiments provided insights into its specific function. The expression pattern of the *NtHDR* was thoroughly analyzed through quantitative real-time PCR analysis. Furthermore, to achieve functional validation, the *NtHDR* was applied into the generation of *Nicotiana benthamiana* via transformation, coupled with the employment of the solid-phase microextraction coupled with gas chromatography–mass spectrometry (SPME-GC-MS) technique. This integrated approach established a solid foundation for delving deeper into the floral metabolism and molecular regulatory mechanisms underlying the captivating flower fragrance of Chinese Narcissus.

2. Materials and Methods

2.1. Plant Materials

The plant material utilized in this study comprised Chinese Narcissus cultivar 'Jinzhanyintai' which was purchased from Zhangzhou, Fujian, China. The plants were cultivated within a controlled artificial climate chamber, maintaining a temperature of 20°C for 14 h of light exposure, as well as a temperature of 16°C for 8 h of darkness, alongside a humidity level of 70%. Figure 1 visually presents the varying stages of 'Jinzhanyintai' flowering. At different time points, the petals, corona, leaves, bulbs, and roots were promptly subjected to snap-freezing in liquid nitrogen and subsequently stored in a -80°C refrigerator for subsequent analysis.

N. benthamiana was grown in a light incubator at 22°C for 22 h of light and 2 h of dark at 50–70% humidity for transient transformation assays.

Preprints (www.preprints.org) | NOT PEER-REVIEWED | Posted: 18 July 2023 doi:10.20944/preprints202307.1182.v1

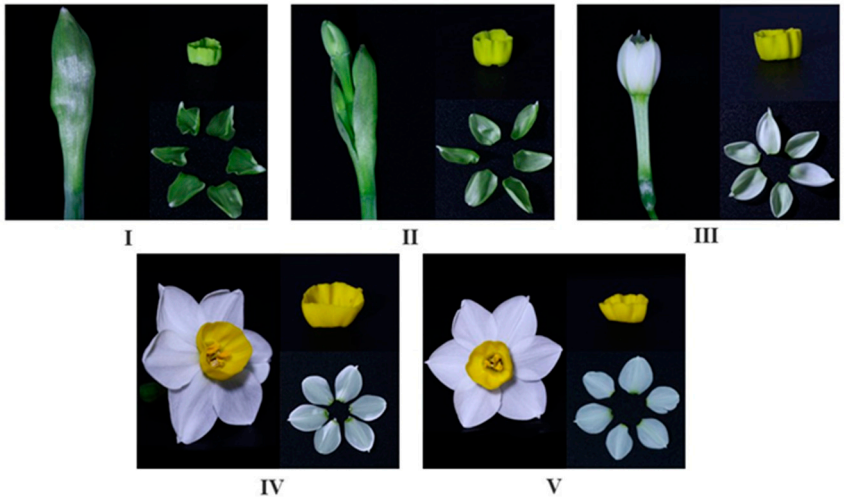

Figure 1. *Narcissus tazetta* 'Jinzhanyintai' in various flowering stages. (I–V) represent the overall state, as well as tissue samples of petals and corona for each of the five distinct periods of 'Jinzhanyintai' flowering.

2.2. Total RNA Extraction and cDNA Synthesis

The total RNA extraction from 'Jinzhanyintai' petals, corona, bulbs, roots, and leaves was performed through the application of the Quick RNA Isolation Kit (0416-50GX, Huayueyang, Beijing, China), according to the manufacturer's instructions. The purity and concentration of the obtained RNA samples were subsequently assessed using NanoDrop2000. For cDNA synthesis, a final reaction volume of 20 μL from total RNA (1 μg) was employed, with the utilization of Oligo(dT)$_{15}$ primers, and AMV Reverse Transcriptase (A3500, Promega, Madison, WI, USA) according to manufacturer's specifications.

2.3. Cloning and Expression Vector Construction of NtHDR

Using the transcriptome sequencing database as a reference, a homology blast analysis was conducted employing the HDR protein sequence from the model plant Arabidopsis thaliana. Subsequently, specific primers were designed following careful screening of the HDR homologous gene sequence (Table 1). Gene coding sequence (CDS) amplification was conducted with applying PrimeSTAR® HS (Premix) (Takara, Kusatsu, Japan). The PCR amplification system and protocol were as follows: PrimeSTAR® HS (Premix, Kusatsu, Japan) 25 μL, 4 μL cDNA template, 2 μL of a 10 μmol·L^{-1} mixture of upstream and downstream primers and supplemented with ddH_2O to a total volume of 50 μL. The amplification procedure was as follows: 95°C for 3 min; 95°C for 15 s, 56°C for 15 s, 72°C for 2 min (35 cycles); 72°C for 5 min; and 4°C +∞. Following PCR, the agarose gel containing the target fragment was excised and purified according to the instructions of the DNA Recovery Kit (DP209, Tiangen, Beijing, China). The purified fragment was then ligated into pCE2 TA/Blunt-Zero Vector (Vazyme, Nanjing, China) and transformed into Escherichia coli DH5α receptor state (CB101, Tiangen, Beijing, China).Positive monoclonal colonies were selected and sent for sequencing to Genewiz. Subsequently, *NtHDR* was ligated to the pBI121 expression vector through the In-Fusion Cloning, with *Xma*I and *Xba*I selected as the enzyme cleavage sites. The enzyme cleavage system and timing were operated according to the instructions provided by BioLab. The homologous amplification primers applied are detailed in Table 2. The PCR amplification system and protocol remained consistent with the aforementioned steps, with the amplification template being the plasmid obtained after correct sequencing in the previous step. The PCR products were recovered by agarose gel purification. The homologous recombination system was prepared following the guidelines outlined in the ClonExpress® II One Step Cloning Kit (Vazyme, Nanjing, China): 200 ng of the digested pBI121 vector, 60 ng of PCR product, 4 μL of 5×CEII Buffer, 2 μL of ExnaseII, and 20 μL of ddH_2O were mixed and incubated at 37°C for 30 min. The resulting mixture was then transferred

Preprints (www.preprints.org) | NOT PEER-REVIEWED | Posted: 18 July 2023 doi:10.20944/preprints202307.1182.v1

into *E. coli* DH5α receptor state. Positive monoclonal colonies were selected and submitted to Genewiz for sequencing.

Table 1. Primers sequences used for PCR.

Primer use	Primer name	Sequences (5′→3′)
Cloning the CDS	*NtHDR*-F	atggcgatggcagttgcag
	NtHDR-R	cgccaactgcatagattcttcc
Subcellular localization analysis	pBI121-*NtHDR*-F	tggagagaacacgggggactatggcgatggcagttgcag
	pBI121-*NtHDR*-R	ataagggactgaccacccgccaactgcatagattcttcc
Stable transformation of *N. benthamiana*	pBI121-*NtHDR*-R2	ataagggactgaccaccttacgccaactgcatagattcttcc
Real-time PCR	*NtActin*-F	tgcccagaagtgctattccag
	NtActin-R	gttgacccaccactaagaacaatg
	qPCR -*NtHDR*-F	tgacgaggggcgataactacaatc
	qPCR -*NtHDR*-R	gactctgctagcttcaccgttac
Identification of positive transgenic *N. benthamiana*	35s-F	gacgcacaatcccactatcc

2.4. NtHDR Bioinformatics Analysis

The structural domain identification of the proteins was analyzed through adopting the NCBI Conserved Domain Search online tool (https://www.ncbi.nlm.nih.gov/). The amino acid composition, protein molecular weight, theoretical isoelectric point (pI), and stability were predicted through utilizing the online software ProtParam tool (http://web.expasy.org/protparam/). The hydrophobic property and charge distribution of the protein were analyzed via the ProtScale tool (https://web.expasy.org/protscale/). To analyze the transmembrane domain of the NtTPS protein, the TMHMM server 2.0 software (http://www.cbs.dtu.dk/services/TMHMM) was employed. The presence of a signal peptide in NtTPS was predicted with the SignalP4.1 Server (http://www.cbs.dtu.dk/services/SignalP/). The tertiary protein structure predictions were conducted through the application of SWISS-MODEL (https://swissmodel.expasy.org/) platforms, respectively. The sequence similarity of comparison was conducted to analyze the *NtHDR* sequence results using BLAST from NCBI [32]. The Neighbor-Joining (NJ) method was employed to construct the phylogenetic tree using MEGA 7.0 software with 1000 bootstrap replicates [33,34].

2.5. Fluorescence Quantification of NtHDR in 'Jinzhanyintai'

Specific amplification primers were designed through applying Primer Premier 6 (Table 1), with primers for reference gene (*Actin*) selected based on previous studies [35]. Moreover, following the manufacturer's recommendation, a LightCycler® 480 fluorescent qPCR instrument and TB Green Premix ExTaqII were utilized for conducting the experiments and the qRT-PCR assays, respectively. Furthermore, each experiment was performed with three technical replicates. The relative expression of the *NtHDR* gene was calculated using the $2^{-\triangle\triangle Ct}$ method[36]. Correlation analysis between the relative expression of the *NtHDR* gene in various periods of Narcissus flowering and in diverse plant parts was performed with SPSS 25.

2.6. Subcellular Localization Assay of NtHDR Proteins in Tobacco

Subcellular localization studies of NtHDR were conducted through the agrobacterium-mediated transient expression technique. The plant overexpression vector plasmid pBI121-*NtHDR*-GFP was transferred into GV3101 agrobacterium tumefaciens competent cells (Shanghai Weidi Biotechnology, Shanghai, China) via heat stimulation. The resulting single colonies were cultured for 60 h and subjected to colony PCR for identification. Positive single colonies were selected and transferred to 20 mL of LB liquid medium containing 50 mg/L kanamycin and 25 mg/L rifampicin, followed by being incubated at 28°C with shaking at 200 rpm until the OD_{600} value reached approximately 0.8 [37].

 doi:10.20944/preprints202307.1182.v1

The bacteria were collected, suspended in a formulation containing 10 mM MES-KOH, 10 mM $MgCl_2$, and 150 μM acetosyringone, and left for 2–3 h. The suspension was injected into N. benthamiana leaves and incubated under low light conditions for 48 h. Subsequently, chloroplast autofluorescence was observed and imaged with a LSM 880 (ZEISS) laser confocal microscope, with an excitation wavelength of 633 nm and an emission wavelength of 684 nm. Additionally, GFP fluorescence was observed and imaged with an excitation wavelength of 488 nm and an emission wavelength of 533 nm [38,39] (Zhang et al., 2022; Liu, 2017). The plant expression vector plasmid pBI121-GFP was utilized as a positive control and treated as pBI121-*NtHDR*-GFP.

2.7. Agrobacterium-Mediated Transformation and Identification of N. benthamiana

The plant overexpression vector plasmid pBI121-*NtHDR* was transferred into GV3101 agrobacterium tumefaciens competent cells through heat stimulation, followed by colony PCR to confirm successful transformation. The subsequent culture procedures were the same as described in Section 4.6. The bacteria were collected, suspended in the MS liquid medium, and allowed to incubate for 2–3 h.

Under aseptic conditions in the ultra-clean table, healthy leaves from well-cultured sterile *N. benthamiana* seedlings were carefully excised into 0.8 cm × 0.8 cm sized leaves (avoiding the veins as much as possible) using sterilized knives. These leaves were then placed onto a culture medium containing MS+6-BA 2.0 mg/L+NAA 0.2 mg/L and kept in the dark for a period of 2 d. Pre-cultured *N. benthamiana* leaves were subsequently immersed in a prepared agrobacterium solution for approximately 10 min, during which the solution was continuously agitated to ensure optimal contact with the leaves. After completion, excess bacterial solution was removed using sterile filter paper, and the leaves were rinsed 2–3 times with sterile water. Subsequently, the leaves were placed on sterile filter paper to dry. A new pre-culture medium was prepared by placing three layers of sterile filter paper in a flat position, and the pre-treated leaves were positioned backside up on the filter paper layers. This setup was maintained in the dark for an additional 2 d. Once adventitious buds started to grow, the leaves were transferred to a normal light condition and the culture medium was changed approximately once every 10 d. The adventitious buds presenting excellent growth were excised and transferred to a differentiation culture medium containing MS+NAA 0.2 mg/L + Kan 100 mg/L + Tim 300 mg/L. For rooting, the adventitious buds were cultured in a 1/2MS+Kan 100 mg/L + Tim 300 mg/L medium until they developed 2–3 leaves and reached sufficient height. Once the root system became adequately grown, the cap of the culture bottle was loosened, and sterile water was added for a period of 3–4 d under low light conditions. Prior to transplanting the seedlings into small plastic pots, the medium on the roots was carefully cleaned, and the seedlings were covered with transparent glass or plastic containers for a period of 10 d after transplantation. This step aimed to maintain a high ambient humidity, allowing the seedlings to gradually adapt to the new environment.

Transgenic *N. benthamiana* DNA was extracted following the protocol outlined in the DNA Extraction Kit (MF735-plus, Juhemei, Beijing, China) to ensure high-quality DNA samples Subsequently, to validate the expression of *NtHDR* at the protein level in the transgenic plants, petals were carefully selected from plants that had been identified as positive for DNA. Moreover, RNA extraction was performed with the RNA Extraction Kit, followed by reverse transcription to synthesize cDNA. The PCR identification process utilized specific primers, namely 35SF and *NtHDR*-R (Table 2), to amplify the target sequence.

2.8. Analysis of Volatile Components in Transgenic N. benthamiana Flowers

Entirely open flowers of transgenic and wild-type *N. benthamiana* were selected with three replicates performed for each assay). The samples were prepared by mixing approximately 0.2 g of randomly selected *N. benthamiana* flowers in a clean 10 mL round-bottomed headspace vial at room temperature (25±2°C). The vial was sealed using a blue Teflon silicone spacer, leaving about 2/3 of the space at the top. Analysis was performed using a 50/30 μm DVB/CAR/PDMS solid-phase microextraction head and HP-5MS (30 m × 250 μm × 0.25 μm) flexible quartz capillary column with

Preprints (www.preprints.org) | NOT PEER-REVIEWED | Posted: 18 July 2023 doi:10.20944/preprints202307.1182.v1

a GC-MS model Agilent 7890A-5975C. The headspace solid-phase microextraction parameters were adjusted based on the work of Sun Miao [40] with appropriate modifications. The aging temperature and time of the extraction head were set at 250°C for 1 h. The extraction process was conducted at 50°C for 30 min, followed by a desorption time of 3 min. The injection port was of the auto injection type. Helium gas was used as the carrier gas, with a column flow rate of 1 mL/min in the pulsed non-split injection mode. The heating temperature of the injection port was maintained at 250°C. For MS analysis, the EI ionization mode was employed, with an electron energy of 70 eV. The ion source and the four-stage rod temperature were set at 230°C and 150°C, respectively. The full scan acquisition mode covered a scan range of 50–600 amu, and the EMV mode was set to the relative value. The equilibration time for the gas phase column chamber was 0.25 min. The ramp-up procedure was as follows: an initial temperature of 55°C held for 3 min, followed by a ramp-up rate of 3°C/min to 148°C for 1 min, then a ramp-up rate of 10°C/min to 210°C for 3 min, and finally a post-run temperature of 55°C for 1 min.

The identification of compounds involved a two-step approach: retention index method and qualitative analysis of volatiles in *N. benthamiana* flowers with the application of the NIST14 spectral library. In addition, manual spectral analysis was performed, taking into account the mass spectra and retention time indexes reported in relevant published literature. This comprehensive analysis facilitated the identification of specific volatile components.

3. Results

3.1. Characterization of NtHDR

The ORF of *NtHDR* spanned 1380 bp, encoding a protein consisting of 460 amino acid residues. The *NtHDR* can be classified under the Isoprenoid_Biosyn_C1 superfamily. The analysis with the ProtParam online tool revealed that the molecular weight of *NtHDR* was approximately 51.38kDa. The theoretical pI of the protein was calculated to be 5.58. Furthermore, the protein instability coefficient was determined to be 32.35, indicating its relatively unstable nature. The mean hydrophilicity (GRAVY) value of -0.372 suggested that *NtHDR* possessed a hydrophilic property (Figure 2C). Prediction analyses conducted through the application of Signa lP4.1 Server and TMHMM indicated the absence of signal peptide sites and transmembrane regions in the *NtHDR* protein, thereby categorizing it as a non-secreted and non-transmembrane protein (Figure 2A and B). To visualize the protein's 3D structure, SWISS-MODEL was utilized, resulting in a model exhibiting approximately 81.21% similarity to the reference model (Figure 2D).

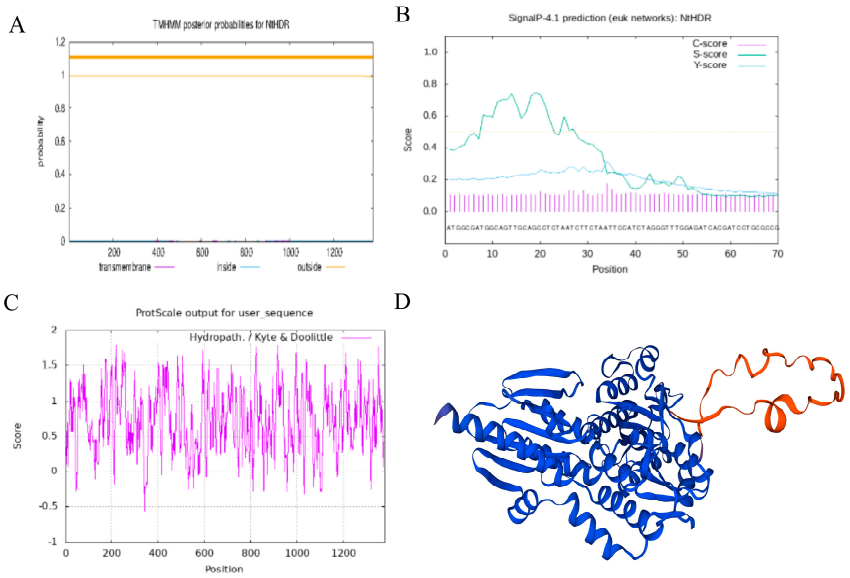

Preprints (www.preprints.org) | NOT PEER-REVIEWED | Posted: 18 July 2023 doi:10.20944/preprints202307.1182.v1

Figure 2. (A) Transmembrane analysis; (B) Signal peptide analysis; (C) Hydrophilic and hydrophobic analysis; (D) Tertiary structure prediction.

3.2. Phylogenetic Analysis and Sequence Alignment of NtHDR

The functional domain analysis revealed that *NtHDR* was attributed to the lytB-ispH superfamily of genes, with the encoded protein exhibiting a highly conserved region. Further analysis of *NtHDR* sequence homology indicated the highest amino acid sequence similarity with *A. officinalis* at 88.35%. Comparatively, *Z. officinale*, *Elaeis guineensis*, *Musa acuminata* subsp. *malaccensis*, and *Ananas comosus* presented 83.97%, 83.3%, 81.03%, and 80.99% gene similarity, respectively (Figure 3). These findings suggested a significant homology of HDR across various species, with strong conservation observed at the C-terminus of the encoded protein. Phylogenetic tree analysis, performed using MEGA7.0 (Figure 4), demonstrated the relationship between HDR genes of 'Jinzhanyintai' and other species. *NtHDR* was found to be closely associated with *A. officinalis* (XP_020241009.1), *Z. officinale* (XP_042395642.1), *Dendrobium officinaleKimura* (AGH62555.1), *Oncidium flexuosum* (ACJ83116.1), *E. guineensis* (XP_010909277.1), *Phoenix dactylifera* (XP_008799160.1), *M. acuminata* subsp. *Malaccensis* (XP_009412299.1), and *A. comosus* (XP_020104485.1), as well as other monocotyledons, forming a closely clustered branch. Notably, the closest relatives were observed to be *A. officinalis* and *Z. officinale*.

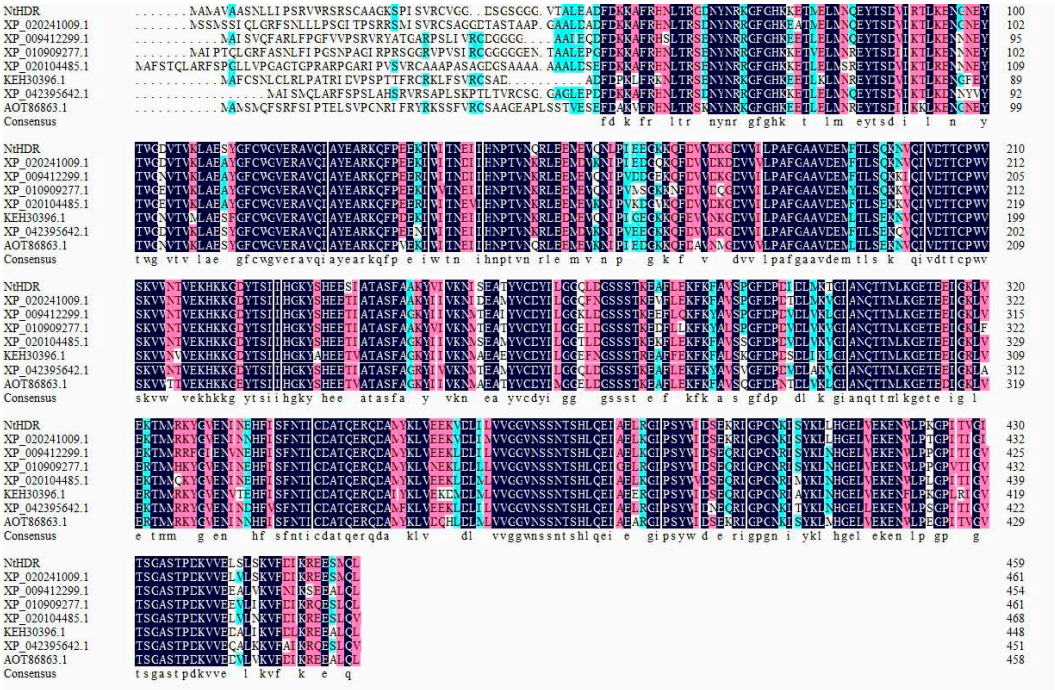

Figure 3. Multiple alignments of HDR amino acid sequences of 'Jinzhanyintai' with those of other species.

Preprints (www.preprints.org) | NOT PEER-REVIEWED | Posted: 18 July 2023 doi:10.20944/preprints202307.1182.v1

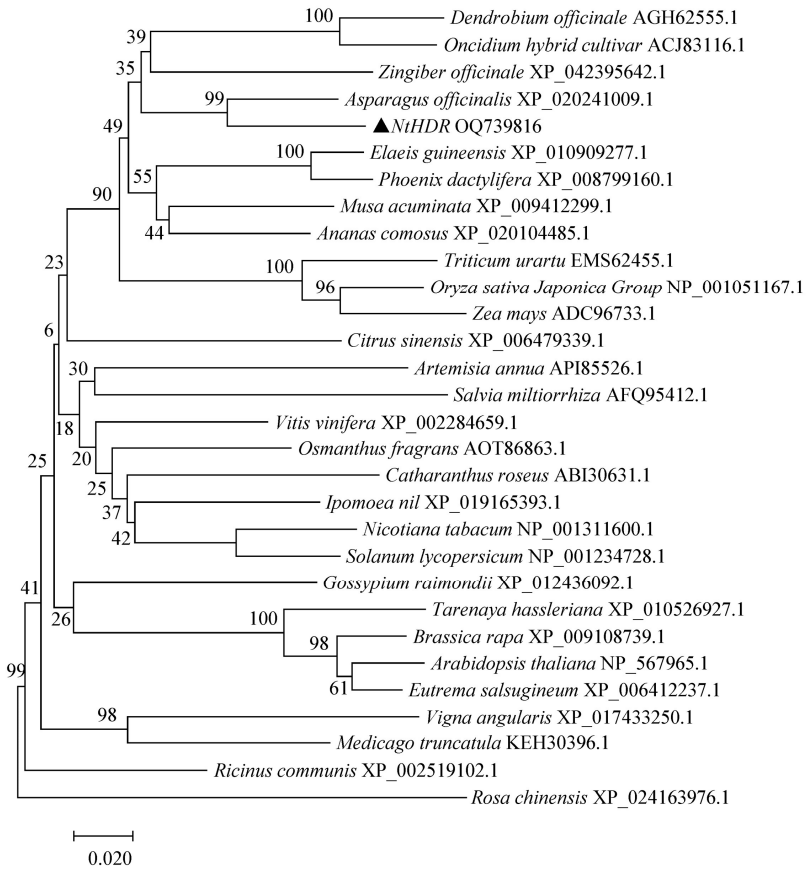

Figure 4. Phylogenetic analysis of NtHDR protein selected from other plant species.

3.3. NtHDR Expression Specificity Analysis

Quantitative real-time fluorescence analysis revealed the expression pattern of NtHDR in various tissues, including petals, corona, leaves, bulbs, and roots, indicating certain variations among them (Figure 5A). Notably, NtHDR exhibited higher expression levels in petals and corona while it presented lower expressions in other tissues, with a ranking order of petals > corona > leaves > roots > bulbs. Moreover, examining the expression level of NtHDR in varying flowering stages revealed interesting trends. In petals, the expression level demonstrated an increasing and then decreasing trend during blooming (Figure 5B), while in the corona, the expression level presented a continuous increasing trend throughout the flowering process (Figure 5C). Overall, the expression pattern of NtHDR demonstrated a regular association with the flowering stage, and the pronounced increase in expression level observed in the corona suggested a potential involvement of NtHDR in the metabolism of floral terpenoids.

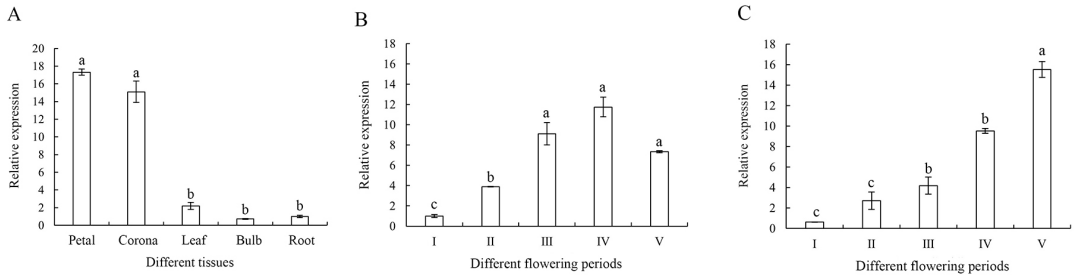

Figure 5. Analysis of relative expression level of NtHDR. (A) Relative expression level of NtHDR in various tissues; (B) Relative expression level of NtHDR at different flowering stages of petals and corona; (C) Relative expression level of NtHDR at different flowering stages of corona; lowercase letters (a, b, and c) indicate significant differences observed between different treatments ($p < 0.05$).

Preprints (www.preprints.org) | NOT PEER-REVIEWED | Posted: 18 July 2023 doi:10.20944/preprints202307.1182.v1

3.4. NtHDR Subcellular Localization Analysis

The pBI121-NtHDR-GFP plasmid-containing Agrobacterium GV3101 strain was infiltrated into N. benthamiana leaves, while the pBI121-GFP plasmid-containing Agrobacterium GV3101 strain served as a control. Subsequent observation by utilizing laser confocal microscopy revealed that the fusion protein of the target gene HDR and GFP generated green fluorescence exclusively on chloroplasts (Figure 6). In the control group, a distinct and bright green fluorescence signal of GFP was identified within the nucleus and cytoplasm, which indicated the localization of NtHDR on chloroplasts. This observation aligned with the knowledge that the MEP pathway, a metabolic pathway involved in floral metabolism, occurred within cellular chloroplasts, as predicted by the website and previous knowledge.

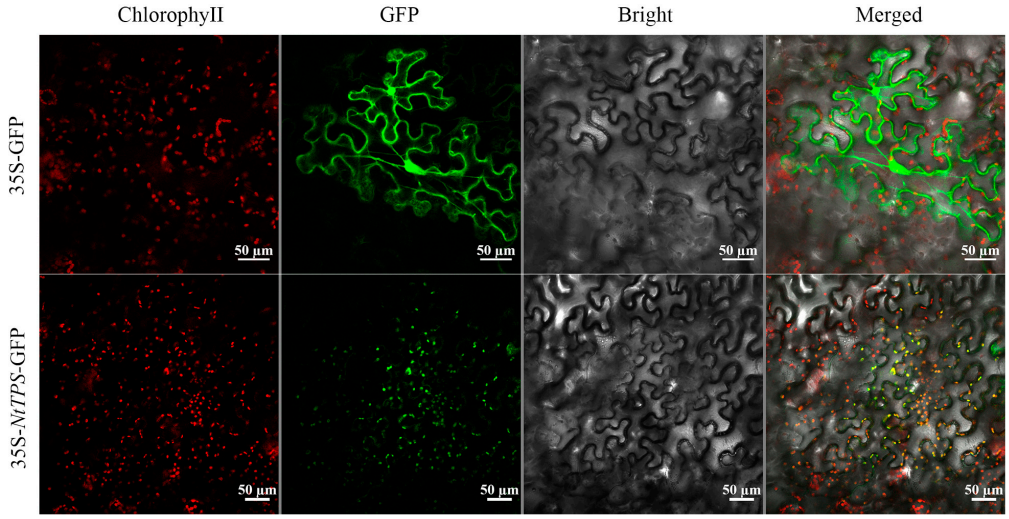

Figure 6. Confocal images of transiently expressed GFP fusions in leaves of N. benthamiana.

3.5. Stable Expression of NtHDR in N. benthamiana

A PCR-based screening method was employed to screen a total of 10 transgenic N. benthamiana plants overexpressing NtHDR, with wild-type plants serving as controls for subsequent investigations (Figure 7). Comprehensive observations, including plant size, leaf morphology, flower color, petal size, and florescence, were conducted on both NtHDR overexpressing N. benthamiana plants and wild-type plants. However, no significant differences were detected between the two groups. The breeding process of transgenic N. benthamiana plants is illustrated in Figure 8 below.

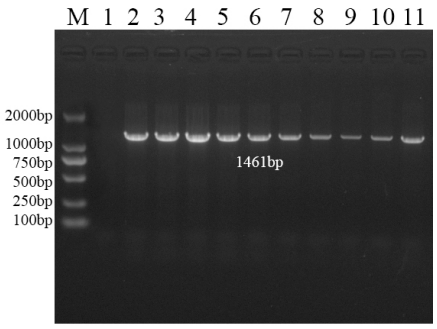

Figure 7. PCR assay of transgenic N. benthamiana plants. M: DL2000 marker; 1: Wild-type N. benthamiana; 2–11: Transgenic N. benthamiana.

Preprints (www.preprints.org) | NOT PEER-REVIEWED | Posted: 18 July 2023 doi:10.20944/preprints202307.1182.v1

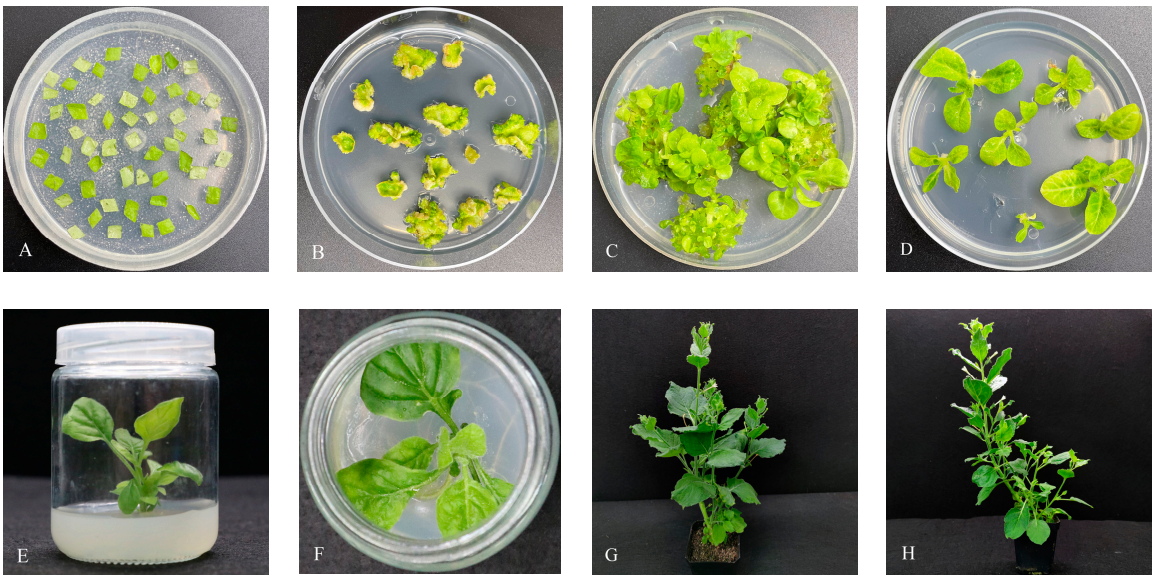

Figure 8. Cultivar of transgenic *N. benthamiana* with pBI121-NtHDR expression vector. The diameter of culture dish is 90 mm, and the diameter and height of culture bottle are 66 mm × 95 mm. (A) Preculturing of wild-type *N. benthamiana*; (B–C) Screening of wild-type *N.benthamiana* with kanamycin; (D) Differentiation culture of *N. benthamiana*; (E–F) Rooting culture; (G) Flowering of transgenic *N. benthamiana*; (H) Flowering of wild-type *N. benthamiana.*

3.6. Determination and Analysis of Floral Volatiles of Transgenic N. benthamiana

Volatile compounds from the flowers of transgenic N. benthamiana plants and wild-type plants were collected using headspace solid-phase microextraction and subsequently analyzed using GC-MS. The analysis revealed discernible differences in the volatile components between the two plant groups(Table 2). Specifically, the transgenic N. benthamiana plants expressing NtHDR exhibited the release of linalool (RT=13.297), benzyl alcohol (RT=10.690), and phenethanol (RT=14.151) as evident in the chromatogram (Figure 9-B). Conversely, these three volatile components were absent in the wild-type plants (Figure 9-A).

Table 2. Main volatile components in fresh flower of different strain *N.benthamiana*.

Main volatile components	Retention time/min	Relative content/%					
		A Wild-type *N. benthamiana*			B Transgenic *N. benthamiana*		
		CK1	CK2	CK3	H1	H2	H3
Benzyl alcohol	10.690	—	—	—	—	1.288	1.687
Phenylacetaldehyde	10.832	1.682	1.001	—	2.652	4.247	1.105
Linalool	13.297	—	—	—	0.551	1.086	0.777
Phenethyl alcohol	14.151	—	—	—	—	1.812	—
Decamethylcyclopentasiloxane	15.963	10.766	10.488	7.715	16.885	12.974	11.461
2-Isobutyl-3-methoxypyrazine	16.893	0.870	—	—	1.003	1.940	—
Cinnamic aldehyde	20.923	3.203	—	0.233	4.047	—	4.133

Preprints (www.preprints.org) | NOT PEER-REVIEWED | Posted: 18 July 2023 doi:10.20944/preprints202307.1182.v1

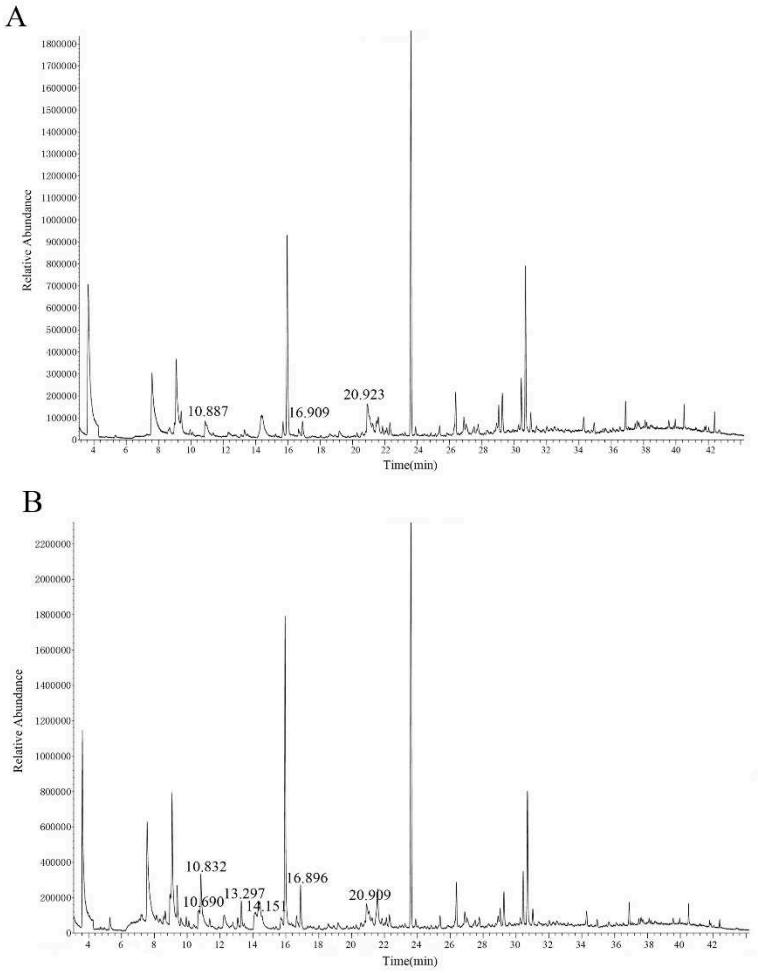

Figure 9. Total ion chromatograms of volatile compounds in fresh flower of different *N. benthamiana* strains. (A) Wild-type *N. benthamiana*; (B) Transgenic *N. benthamiana* with pBI121-NtHDR expression vector. The unlabeled spurious peak is the extractor head coating off.

4. Discussion

In this study, we cloned an HDR enzyme gene from Chinese Narcissus 'Jinzhanyintai' and successfully introduced it into *N. benthamiana* plants to achieve stable transformation. The floral fragrance components of the transgenic plants were investigated using SPME-GC-MS. Our analysis revealed the presence of the monoterpene volatile linalool, as well as the phenylpropanoids benzyl alcohol and phenylethanol, in the *NtHDR* overexpression plants, whereas these components were undetectable in the wild-type plants. In addition, our findings align with previous research conducted by Pang Hongdong [29] who transferred the SAMT enzyme gene serving as a key component in the metabolic pathway of phenylpropanoids/phenylcyclic compounds in Rhamnus phyllanthus into *N. tabacum*. Pang Hongdong observed higher levels of hexenal, benzyl alcohol, and linalool, while methyl benzoate was not detected. The author hypothesized that the introduction of *CpSAMT* may have disrupted the synthesis pathway of methyl benzoate in *N. benthamiana*, thereby leading to more accumulation of benzyl alcohol. Hence, considering the outcomes of our study, we speculated that the production of linalool, benzyl alcohol, and phenylethanol may suggest an unknown association between the phenylpropanoid/phenylcyclic compound metabolic pathway and the terpene metabolic pathway. However, due to the incomplete understanding of the phenylpropanoid/phenylcyclic compound metabolic pathways, further investigations are necessary to elucidate the specific mechanisms underlying their interplay with terpene metabolic pathways. Furthermore, Zhang Tengxun [30] transferred the DXS enzyme gene, an essential component of the MEP pathway in Lilium brownii, into *N. tabacum* and observed significantly higher linalool content in the transgenic flowers compared to wild-type plants. Similarly, in our experiment, the introduction

of the key enzyme gene HDR from the MEP pathway into *N. benthamiana* resulted in increased linalool content in the transgenic plants' flowers. Chen Jindou [31] transferred the putative phenylpropane transcription factor *CpODORANT* into *N. tabacum* and suggested that the monoterpene ocimene was only present in the control and wild-type *N. tabacum* flowers, whereas it could not be detected in the flowers of transgenic *CpODORANT N. tabacum.* Conversely, a small amount of sesquiterpenes geraniene and germacrene D were produced. This observation may help explain the complexity of the floral aroma regulation mechanism in *N. tabacum*. Based on the aforementioned findings, we inferred that the overexpression of *NtHDR* in *N. benthamiana* plants led to increased accumulation of IPP and DMAPP, the floral precursor substances in the MEP pathway. Consequently, this upregulation affected the downstream formation of the monoterpene compound linalool, as well as the phenylpropanoid metabolic pathway in *N. benthamiana*, resulting in the production of benzyl alcohol and phenylethanol. Overall, our findings provide preliminary evidence supporting the significant regulatory role of the HDR gene in the floral metabolic pathway at the transgenic level.

5. Conclusions

In this study, HDR, a key enzyme gene located at the end of the MEP pathway, was cloned from the petals of Nar. tazetta var. chinensis 'Jinzhanyintai' and named *NtHDR*. *NtHDR* played a role in the floral biosynthesis process and was capable of promoting the synthesis of terpene volatiles.

Author Contributions: Conceptualization, Meng Hu, Tao Hu and Jun Ma; Data curation, Meng Hu, Na Zhang and Yun Deng; Formal analysis, Meng Hu and Na Zhang; Investigation, Meng Hu, Na Zhang, Bo Zhang and Hua Wang; Methodology, Meng Hu, Na Zhang, Yan Chang, Yun Deng, Tao Hu and Jun Ma; Resources, Meng Hu, Na Zhang, Yan Chang and Bo Zhang; Software, Meng Hu, Na Zhang and Ke Fan; Supervision, Meng Hu; Validation, Meng Hu and Na Zhang; Visualization, Meng Hu; Writing – original draft, Meng Hu and Na Zhang; Writing – review & editing, Meng Hu and Na Zhang.

Funding: This research was supported by ICBR Fundamental Research Funds Grant (NO. 1632020021 and NO. 1632022013).

Data Availability Statement: All data in this study could be found in the manuscript

Acknowledgments: We thank all the colleagues that helped with the development of different parts of this manuscript and the State Key Laboratory of Tree Genetics and Breeding for providing equipment and technical support for this study.

Conflicts of Interest: The authors declare no conflict of interest.

References

1. Pichersky, E.; Noel, J.P.; Dudareva, N. Biosynthesis of plant volatiles: Nature's diversity and ingenuity. *Science*, **2006**, *311*, 808–811. https://doi.org/10.1126/science.1118510.
2. Kessler, A.; Baldwin, I.T. Defensive function of herbivore-induced plant volatile emissions in nature. *Science*, **2001**, *291*, 2141–2144. https://doi.org/10.1126/science.291.5511.2141.
3. Chen, F.; Tholl, D.; Bohlmann, J.; Pichersky, E. The family of terpene synthases in plants: A mid-size family of genes for specialized metabolism that is highly diversified throughout the kingdom. *Plant J*, **2011,** *66*, 212–229. https://doi.org/10.1111/j.1365-313X.2011.04520.x.
4. Dudareva, N.; Klempien, A.; Muhlemann, J.K.; Kaplan, I. Biosynthesis, function and metabolic engineering of plant volatile organic compounds. *New Phytol*, **2013**, 198, 16–32. https://doi.org/10.1111/nph.12145.
5. Kitaoka, N.; Lu, X.; Yang, B.; Peters, R. J. The application of synthetic biology to elucidation of plant mono-, sesqui-, and diterpenoid metabolism. *Mol. Plant* , **2015**, *8*, 6–16. https://doi.org/10.1016/j.molp.2014.12.002.
6. Vranová, E.; Coman, D.; Gruissem, W. Network analysis of the MVA and MEP pathways for isoprenoid synthesis. *Annu. Rev. Plant Biol*. **2013**, *64*, 665–700. https://doi.org/10.1146/annurev-arplant-050312-120116.
7. Zhang, Y.T.; Cui, J.B.; Hu, H.L.; Xue, J.Y.; Yang, J.J.; Xu, J. Integrated four comparative-omics reveals the mechanism of the terpenoid biosynthesis in two different overwintering Cryptomeria fortunei phenotypes. *Front. Plant Sci*, **2021**, *12*, 740-755. https://doi.org/10.3389/fpls.2021.740755.
8. Adam, P.; Hecht, S.; Eisenreich, W.; Kaiser, J.; Gräwert, T.; Arigoni, D.; Bacher, A.; Rohdich, F. Biosynthesis of terpenes: Studies on 1-hydroxy-2-methyl-2-(E)-butenyl 4-diphosphate reductase. *Proc. Natl. Acad. Sci. U. S. A*, **2002**, *99*, 12108–12113. https://doi.org/10.1073/pnas.182412599.

9. Altincicek, B.; Duin, E.C.; Reichenberg, A.; Hedderich, R.; Kollas, A.K.; Hintz, M.; Wagner, S.; Wiesner, J.; Beck, E.; Jomaa, H. LytB protein catalyzes the terminal step of the 2-C-methyl-D-erythritol-4-phosphate pathway of isoprenoid biosynthesis. *FEBS Lett*, **2002**, *532*, 437–440. https://doi.org/10.1016/S0014-5793(02)03726-2.
10. Wolff, M.; Seemann, M.; Tse Sum Bui, B.; Frapart, Y.; Tritsch, D.; Garcia Estrabot, A.; Rodríguez-Concepción, M.; Boronat, A.; Marquet, A.; Rohmer, M. Isoprenoid biosynthesis via the methylerythritol phosphate pathway: The *(E)*-4-hydroxy-3-methylbut-2-enyl diphosphate reductase (LytB/IspH) from Escherichia coli is a [4Fe-4S] protein. *FEBS Lett*, **2003**, *541*, 115–120. https://doi.org/10.1016/S0014-5793(03)00317-X.
11. Botella-Pavía, P.; Besumbes, Ó.; Phillips, M.A.; Carretero-Paulet, L.; Boronat, A.; Rodríguez-Concepción, M. Regulation of carotenoid biosynthesis in plants: Evidence for a key role of hydroxymethylbutenyl diphosphate reductase in controlling the supply of plastidial isoprenoid precursors. *Plant J*, **2004**, *40*, 188–199. https://doi.org/10.1111/j.1365-313X.2004.02198.x.
12. Page, J.E.; Hause, G.; Raschke, M.; Gao, W.Y.; Schmidt, J.; Zenk, M.H.; Kutchan, T.M. Functional analysis of the final steps of the 1-deoxy-D-xylulose 5-phosphate (DXP) pathway to isoprenoids in plants using virus-induced gene silencing. *Plant Physiol*, **2004**, *134*, 1401–1413. https://doi.org/10.1104/pp.103.038133.
13. Hao, G.P.; Shi, R.J.; Tao, R.; Fang, Q.; Jiang, X.Y.; Ji, H.W.; Feng, L.; Huang, L.Q. Cloning, molecular characterization and functional analysis of 1-hydroxy-2-methyl-2-(E)-butenyl-4-diphosphate reductase (HDR) gene for diterpenoid tanshinone biosynthesis in *Salvia miltiorrhiza* Bge. f. alba. *Plant Physiol. Biochem,* **2013**, *70*, 21–32. https://doi.org/10.1016/j.plaphy.2013.05.010.
14. Wu, Q.J.; Wu, M.J.; Wang, X.; Lin, Y.; Cai Y.P.; Fan, H.H. Cloning and expression analysis of 1-hydroxy-2-methyl-2-(E)-butenyl-4-diphosphatereductase gene in *Dendrobium officinale*. *Chinese Traditional and Herbal Drugs,* **2015**, *46*, 405–411. (in Chinese)
15. Jiang, Z.; Peng, Z. Chinese Narcissus; China Forestry Publishing House: Beijing, China, 2014; ISBN 978-75-0386-911-2.
16. Gao, J. The study on mutagenic effects and mechanism of ^{60}CoY-ray on Chinese narcissus. *Chinese Academy of Forestry, Beijing*, **2000**.
17. Peng, A.M. Analysis on volatile components of *Narcissus tazetta* var. *chinensis* and influence factors. *Chinese Academy of Forestry*, Beijing, 2010. (in Chinese)
18. Dai, L.; Yang, L.; Guo Y.; Peng Q. Study on the chemical composition of the essential oil of *Narcissus tazetta* var. *chinensis*. *Chromatography*, **1990**, *6*, 377–380. (in Chinese)
19. Huang, Q.Q.; Feng, J.Y. Study of aroma changes in daffodils by adsorption filament/chromatography/mass spectrometry. *Chinese Journal of Analytical Chemistry*, **2003**, *31*, 1408. (in Chinese)
20. Huang, Q.Q.; Feng, J.Y. Study on the variation in narcissus aroma composition during blossoming. *Journal of Instrumental Analysis*, **2004**, 23, 110–113. (in Chinese)
21. Dou, Y.J.; Zhai, J.; Hou, F.M.; Leng, P.S.; Wang, W.F.; Hu, Z.H. Effect of Different Light Intensities on the Floral Aroma Emitted from Chinese Daffodil (*Narcissus tazetta* L. var. *chinensis* Roem). *Acta Agriculturae Boreali-Occidentalis Sinica,* **2014**, *23*, 85–91. (in Chinese)
22. Song, G.; Xiao, J.; Deng, C.; Zhang, X.; Hu, Y. Use of solid-phase microextraction as a sampling technique for the characterization of volatile compounds emitted from Chinese daffodil flowers. *J. Anal. Chem*, **2007**, *62*, 674–679. https://doi.org/10.1134/S1061934807070118.
23. Wu, Y. Study on Cloning of HDS gene and resistant transcription factor of *Narcissus tazetta*. *Fujian Agriculture and Forestry University*, Fuzhou, **2016**. (in Chinese)
24. Zhong, X. The study ofrelationship of B-glucosidase andvolatile aromatic components of *Narcissus tazetta* L. var. *Chinensis* Roem. *Fujian Agriculture and Forestry University*, Fuzhou, **2014**. (in Chinese)
25. Zheng, Q.B. Clone of the *NtSAMT* Gene in *Narcissus tazetta* L. Var. *chinensis* roem and transformation of *Asarina procumbens*. *Northeast Agricultural University*, Haerbin, **2016**. (in Chinese)
26. Li, K. Fragrance component analysis and genecloning in *Narcissus tazetta*. *Fujian Agriculture and Forestry University*, Fuzhou, **2014**. (in Chinese)
27. Ma, C. Cloning of DXPS, DXR and PAL related to floral fragrance from *Narcissus tazetta* L. var. *chinensis* Roem. *Fujian Agriculture and Forestry University*, Fuzhou, **2010**. (in Chinese)
28. Li, L. Analysis of genes related to the terpenoids synthesis pathway in *Narcissus tazetta* 'Yunxiang' based on Transcriptome data. *Fujian Agriculture and Forestry University*, Fuzhou, **2019**. (in Chinese)
29. Pang, H.D.; Xiang, L.; Zhao, K.G.; Li, X.; Yang, N.; Cheng, L.Q. Genetic transformation and functional characterization of Chimonanthus praecox SAMT gene in tobacco. *Journal of Beijing Forestry University*, **2014**, *36*, 117–122. (in Chinese)
30. Zhang, T. Molecular cloning and functional analysis of the key enzyme *LiDXS* genes involved in monoterpene biosynthesis in lily. *Beijing Forestry University*, Beijing, **2017**. (in Chinese)
31. Chen, J.D. Founction research of odorant in *chimonanthus praecox*. *Central China Agricultural University*, Wuhan, **2016**. (in Chinese)

32. Altschup, S.F.; Gish, W.; Miller, W.; Myers, E.W.; Lipman, D.J. Basic local alignment search tool. *J. Mol. Biol*. **1990**, *215*, 403-410. https://doi.org/10.1016/S0022-2836(05)80360-2.
33. Kumar, S.; Stecher, G.; Tamura, K. MEGA7: Molecular evolutionary genetics analysis version 7.0 for bigger datasets. *Mol. Biol. Evol*, **2016**, *33*, 1870–1874. https://doi.org/10.1093/MOLBEV/MSW054.
34. Saitou, N.; Nei, M. The neighbor-joining method: A new method for reconstructing phylogenetic trees. *Mol. Biol. Evol*, **1987**, 4, 406–425. https://doi.org/10.1093/oxfordjournals.molbev.a040454.
35. Wang, G. Transcriptome analysis of flowers and functional studies of MYB genes offlavonoid biosynthetic pathway in Chinese narcissus (*Narcissus tazetta* var. *chinensis*). *Fujian Agriculture and Forestry University*, Fuzhou, **2018**. (in Chinese)
36. Livak, K.J.; Schmittgen, T.D. Analysis of relative gene expression data using real-time quantitative PCR and the $2^{-\Delta\Delta CT}$ method. *Methods*, **2001**, *25*, 402–408. https://doi.org/10.1006/meth.2001.1262.
37. Meng, N.; Liu, Y.L.; Dou, X.X.; Liu, H.L.; Li, F.Y. Transient gene expression in Phalaenopsis aphrodite petals via Agrobacterium tumefaciens infiltration. *Acta Botanica Boreali-Occidentalia Sinica*, **2018**, *38*, 1017–1023. (in Chinese)
38. Zhang, C.G.; Ge, Y.Y.; Liu, H.H.; Zong, Y.X.; Wu, X.J.; Yang, L.C.; Li, H.G. Cloning and bioinformatics analysis of *LtuHMGS* in *Liriodendron tulipifera*. *Journal of Central South University of Forestry & Technology*, **2022**, *42*, 146–155. (in Chinese)
39. Liu, G. Differential regulation of catechin metabolism in albino and normal tea (*Camellia sinensis*) leaves and tea linalool biosynthesis. *Anhui Agricultural University*, Hefei, **2017**. (in Chinese)
40. Sun, M. Cloning and functional analysis of TPS gene family in tree peony fragrance. *Beijing Forestry University*, Beijing, **2021**. (in Chinese)